

Characterizing correlations and synchronization in collective dynamics

Carlos Aguirre *

GNB, Escuela Politécnica Superior,
Universidad Autónoma de Madrid, Campus de Cantoblanco,
Ctra de Colmenar Km 16, 28049 Madrid, Spain

R. Vilela Mendes †‡

CMAF, Universidade de Lisboa,
Faculdade de Ciências C6, 1749-016 Lisboa, Portugal
IPFN, Instituto Superior Técnico,
Av. Rovisco Pais 1, 1049-001 Lisboa

Abstract

Synchronization, that occurs both for non-chaotic and chaotic systems, is a striking phenomenon with many practical implications in natural phenomena. However, even before synchronization, strong correlations occur in the collective dynamics of complex systems. To characterize their nature is essential for the understanding of phenomena in physical and social sciences. The emergence of strong correlations before synchronization is illustrated in a few piecewise linear models. They are shown to be associated to the behavior of ergodic parameters which may be exactly computed in some models. The models are also used as a testing ground to find general methods to characterize and parametrize the correlated nature of collective dynamics.

Keywords: Correlation; Synchronization; Collective dynamics

1 Introduction

Synchronization in complex systems [1] [2] [3] [4] [5] [6] [7] is a striking cooperative phenomena in Nature that has been shown to be of fundamental importance in fields as diverse as the operation of heart pacemaker cells [8] [9], circadian cycles [10], epileptic seizures [11] [12], schizophrenia disorders [13] [14], neuronal firing [15] [16] [17], animal behavior [18], social fads, the integration of cognitive

*e-mail: carlos.aguirre@uam.es

†e-mail: rvilela.mendes@gmail.com

‡Corresponding author

tasks [19] [20] [21], synchronization-based computation [22] and even quantum systems [23].

Many natural systems can be described as networks of oscillators coupled to each other. Coupled oscillators may display synchronized behavior, i.e. follow a common dynamical evolution. Synchronization properties are dependent on the coupling pattern among the oscillators, represented as an interaction network [24] [25] [26] [27] [28] [29] [30] [31] [32]. The central question concerns the emergence of coherent behavior: synchronization or other types of correlation. This occurs both for systems with regular behavior as well as for systems which have chaotic dynamics (lasers, neural networks, physiological processes, etc.). Chaotic systems are characterized by a strong sensitivity to initial conditions, and two identical uncoupled chaotic systems will become uncorrelated at large times even if they start from very similar (but not identical) states. Nevertheless, the coupling of such systems can make them follow the same chaotic trajectories [33] [34] [35] [36] [37] [38].

The degree of synchronization is usually measured by a parameter related to the coherence of the phases or by the entropy of the phases distribution [39]. Most of the work developed so far in this field has emphasized criteria for synchronizability and the relation between network structure and the emergence of synchronized behavior. Typically, the emphasis has been on the distinction between synchronized and incoherent behavior or on their coexistence as in the so-called chimera states [40] [41] [42] [43] [44] [45]. Some exploration, mostly numerical, has also been done on partially synchronized states, clustering, dimensional reduction, etc [46] [47] [48] [49] [50] [51] [52] [53]. However little has been done on the way of developing effective tools to characterize, in a quantitative manner, the striking correlation phenomena that may appear before synchronization or even in the apparently incoherent phases of some systems. That is the main purpose of this work.

As a first step we have started to identify a set of models which, while representative of the actual situations found in the natural world, were also sufficiently simple to provide an identification of the mechanisms underlying the correlation and synchronization phenomena. This search led to the choice of:

- A) A deformed Kuramoto model,
- B) A model of coupled oscillators with a triangle interaction,
- C) An integrate-and-fire model.

The first two models are representative of the stylized behavior found in many collective systems in biology, population dynamics, socio-economic phenomena, etc. In addition, the first model has in some limit a complete characterization of the Lyapunov spectrum, which provides a good hint on the relevance of the ergodic invariants to collective behavior. Finally the third model relates to neuroscience.

Once these models studied, mostly by numerical simulation, we have tested whether simple correlation tools might be sufficient to unravel the correlation behavior that arises before synchronization. Having these tests, partly described in subsection 2.1, shown that the usual correlation measures are not sufficient

for our purposes, we set out to develop new tools which are described in section 3 and tested on the models in section 4. Admittedly, the new tools are more complex than simple correlations. Nevertheless they are not hard to program and even implement as an automatic diagnostic.

2 The models

2.1 A deformed Kuramoto model

The main model used, in the past, for the study of synchronization phenomena was the Kuramoto model [54]

$$\frac{d\theta_i}{dt} = \omega_i + \frac{K}{N-1} \sum_{j=1}^N \sin(\theta_j - \theta_i) \quad (1)$$

The analysis of the Kuramoto model has a long history, with a number of important results obtained throughout the years [55] [56] but a full understanding of its dynamics is still lacking, and most of the rigorous results are only strictly valid in the thermodynamic limit.

Here we use a model of the same type. This model, first mentioned in [57], is

$$x_i(t+1) = x_i(t) + \omega_i + \frac{K}{N-1} \sum_{j=1}^N \pi f^{(n)}(x_j - x_i) \quad (\text{mod } \pi) \quad (2)$$

with $x_i \in [-\pi, \pi)$ and $f^{(n)}$ a deformed version of the Kuramoto interaction

$$f^{(n)}(x) = \text{sign}(x) \left(\sin \left(\frac{|x|^n}{\pi^{n-1}} \right) \right)^{1/n} \quad (3)$$

For $n=1$ $f^{(1)} = \sin(x)$ and when $n \rightarrow \infty$ it becomes (Fig. 1)

$$f^{(\infty)}(x_j - x_i) = \frac{1}{\pi} (x_j - x_i) \quad (\text{mod } 1) \quad (4)$$

For the numerical examples the ω_i 's will follow a Cauchy distribution

$$p(\omega) = \frac{\gamma}{\pi [\gamma^2 + (\omega - \omega_0)^2]} \quad (5)$$

The $f^{(\infty)}$ interaction will be used to derive parameters that characterize the correlations that emerge before synchronization. However they can also be easily computed in more general systems.

For coupled dynamical systems, an order parameter for synchronization is, for example [58]

$$R_n(t) = \left| \sum_{m=1}^N A_{n,m} e^{ix_m(t)} \right| \quad (6)$$

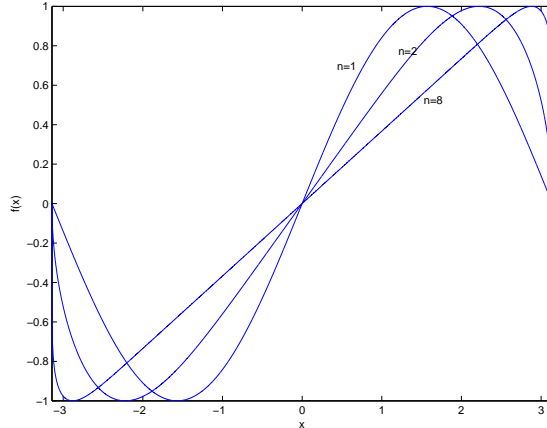


Figure 1: The $f^{(n)}$ interaction function

where A is the adjacency matrix. For the fully coupled system we consider, it is simply

$$r(t) = \left| \frac{1}{N} \sum_{j=1}^N e^{ix_j(t)} \right| \quad (7)$$

In the Figs. 2, 3 and 4 we display the results of numerical simulation of the system (2) with $f^{(\infty)}$, $N = 100$, $K = 0.2$, $K = 0.4$ and $K = 0.8$. A typical distribution of the Cauchy-distributed frequencies ω_i is plotted in Fig.5. We start from random initial conditions and plot the color-coded coordinates $x_i(t)$ from $t = 500$ to $t = 600$. One sees that for the small K the coordinates seem to be uncorrelated whereas for larger K a large degree of synchronization is observed. This is also the information that one obtains from the behavior of the order parameter $r(t)$.

The behavior of the model is similar to Kuramoto's. An important question is whether synchronization is all there is in the dynamics of interacting oscillators. In the past, several authors have found, for example, synchronized cluster formation, before the full synchronization transition. The simplicity of the present model allows for further exploration of this question and a useful hint is, as usual, obtained from the computation of the ergodic parameters [59]. In particular the Lyapunov spectrum of model (2), in the $n \rightarrow \infty$ case, may be obtained exactly.

When $K = 0$ there are N neutral directions, that is, the effective dynamical dimension is N and the Lyapunov spectrum contains N zeros. However, as soon as $K > 0$, the Lyapunov spectrum consists of one isolated zero and $\log\left(1 - \frac{N}{N-1}K\right)$, $(N-1)$ -times. Therefore although it is only for sufficiently large K that synchronization effects seem to occur, there are, for any small $K > 0$, $N-1$ contracting directions. The effective dynamical dimension is one for any small $K > 0$. As soon as there is a (positive) interaction between

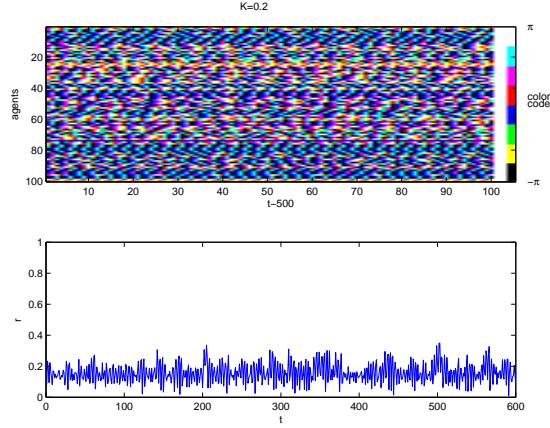


Figure 2: Coordinates x_i and order parameter $r(t)$ for $K = 0.2$

the units, they are, in the ergodic sense, enslaved to a single collective dynamics. Notice that this is not a pathology of this model. Numerical simulation of the Kuramoto and other models also show a drastic reduction of the effective dimension before the synchronization transition.

The fact that the Lyapunov spectrum of the deformed Kuramoto model in the $n \rightarrow \infty$ limit may be obtained exactly, provides important information on the mechanisms that occur before and at synchronization. The eigenvectors of the Jacobian are

$$\begin{pmatrix} 1 \\ 1 \\ 1 \\ \vdots \\ \vdots \\ \vdots \\ 1 \end{pmatrix}; \begin{pmatrix} 1 \\ -1 \\ 0 \\ \vdots \\ \vdots \\ 0 \end{pmatrix}; \begin{pmatrix} 1 \\ 1 \\ -2 \\ 0 \\ \vdots \\ 0 \end{pmatrix}; \dots; \begin{pmatrix} 1 \\ 1 \\ 1 \\ 1 \\ \vdots \\ -N+1 \end{pmatrix}$$

the first one being associated to the eigenvalue 1 and all the others to $\left(1 - \frac{N}{N-1}K\right)$. Denoting by x_i the agents coordinates, the eigenmodes associated to these eigenvectors are

$$Y_{N,p} = \sum_{i=n}^{n+p-1} x_i - px_{n+p}$$

For $K \neq 0$ and before synchronization these modes follow complex periodic orbits which converge to fixed points when synchronization sets in. Therefore one finds here two distinct phenomena. The first one is the dimension reduction at $K = 0$ and then the convergence to fixed points of the eigen-motions associated to the negative Lyapunov exponents. Here the dimension reduction threshold is quite sharp at $K = 0$, but in other models it is more gradual.

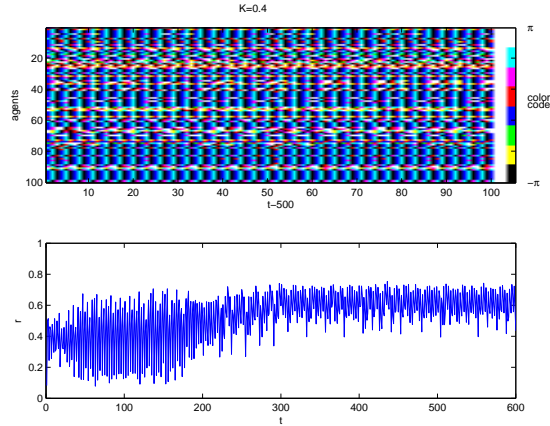


Figure 3: Coordinates x_i and order parameter $r(t)$ for $K = 0.4$

The synchronization order parameter (7) cannot by itself describe the strong correlations and dimensional reduction that occur before synchronization. As shown for the simple model (2) in the $n \rightarrow \infty$ limit, characterization of the correlations may be obtained by the projections on the eigenvectors of the Lyapunov matrix. However our aim is to develop general methods that might be applied to any system when one has no access to its solutions or even to the equations that generate the time series. Will a correlation measure be sufficient to unravel all the complexities that arise before synchronization? To explore this possibility we have computed the correlation of the agents dynamics. That is, we have computed the increments of the coordinates (on the circle), for a long time interval, and from them the matrix of correlations. A typical example is shown in Fig.6 with the same colour code as Fig.2 for positive correlation and black for zero or negative correlation.

In the figure, at $K = 0.2$, one sees many different correlations of several intensities. However it is not clear, from examination of this figure, how to characterize the nature of the correlations nor how they evolve as one approaches the synchronization regime. This has led us to propose several other methods which were then tested on the models: One is based on the geometrical characterization of the dynamics, another is related to dynamical clustering using spectral methods and another one is based on a version of the notion of conditional Lyapunov exponents.

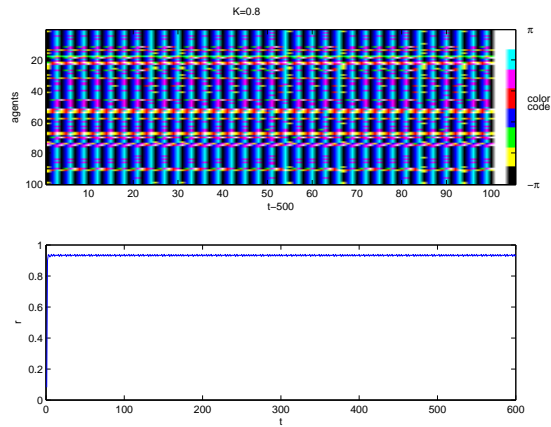


Figure 4: Coordinates x_i and order parameter $r(t)$ for $K = 0.8$

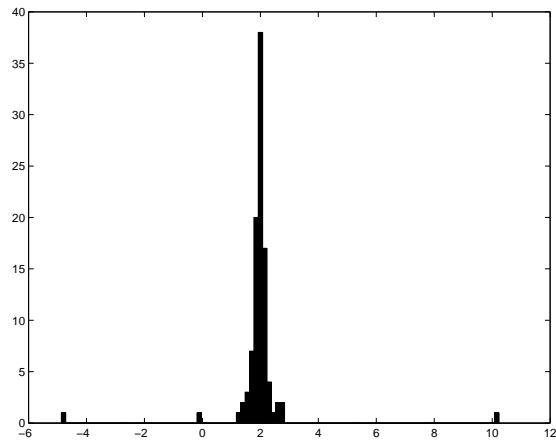


Figure 5: A typical distribution of the Cauchy-distributed frequencies ω_i

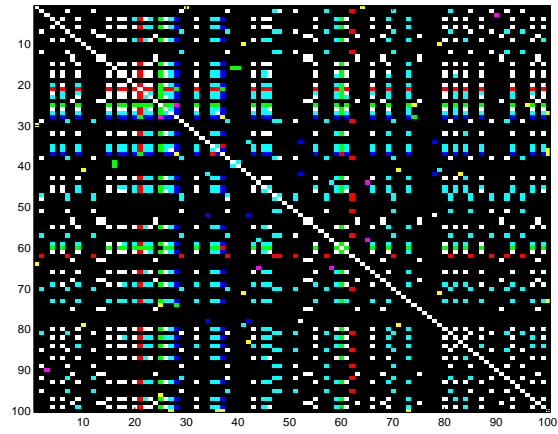


Figure 6: The agents' correlation matrix for the deformed Kuramoto model when $n \rightarrow \infty$ and $K = 0.2$

2.2 Coupled oscillators with a triangle interaction

Here the dynamical law is

$$x_i(t+1) = x_i(t) + \omega_i + \frac{K}{N-1} \sum_{j=1}^N g(x_j - x_i) \quad (\text{mod } \pi) \quad (8)$$

$g(x)$ being the function displayed in Fig.7. The frequencies ω_i are also assumed to follow a Cauchy distribution.

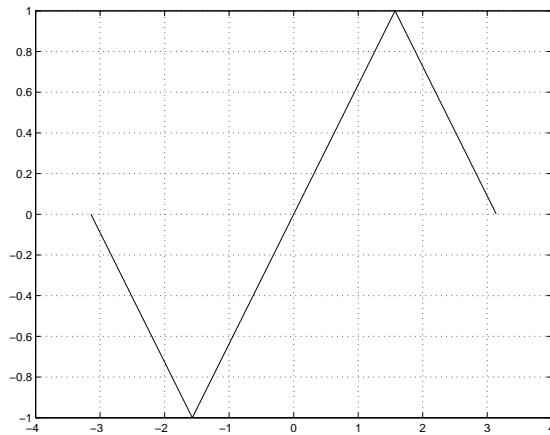


Figure 7: The "triangle" function

As in the previous example, for small values of the coupling (K) the order parameter r fluctuates around small values, whereas for large values the synchronization is apparent (Figs.8, 9 and 10)

However, one sees by computing numerically the Lyapunov spectrum (Fig.11), that already for very small K values, instead of N neutral directions there are a number of contracting directions, implying a reduction in the effective dimension. This is not apparent on the behavior of the order parameter r , emphasizing once more the need to characterize the correlations that appear before synchronization.

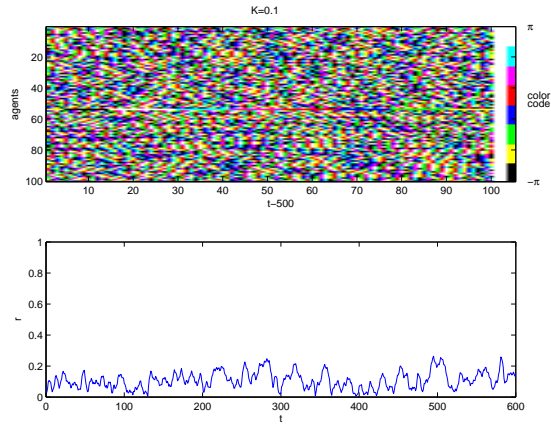


Figure 8: Coordinates x_i and order parameter $r(t)$ for $K = 0.1$ (triangle interaction)

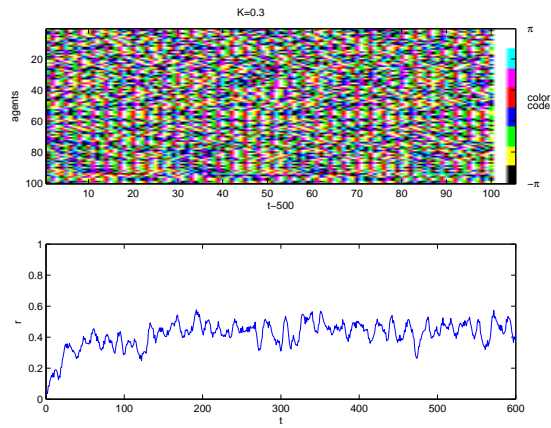


Figure 9: Coordinates x_i and order parameter $r(t)$ for $K = 0.3$ (triangle interaction)

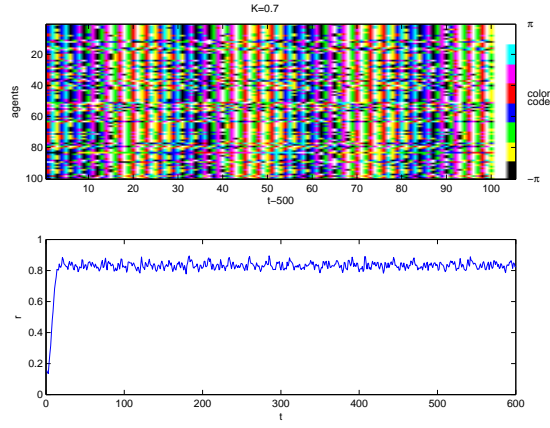


Figure 10: Coordinates x_i and order parameter $r(t)$ for $K = 0.7$ (triangle interaction)

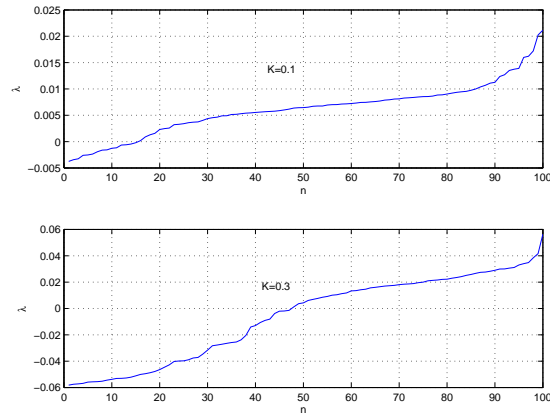


Figure 11: Numerically computed Lyapunov spectrum for the triangle interaction at $K = 0.1$ and $K = 0.3$

2.3 A deterministic "integrate and fire" model

Our third example is of a different nature from the previous ones. The dynamics is defined by

$$x_i(t+1) = x_i(t) + s_i + \frac{k}{N-1} \sum_{j \neq i} \theta(x_j(t-1) - x_j(t) - 0.4) \quad (\text{mod}1) \quad (9)$$

θ being the function

$$\begin{cases} x > 0 & \theta(x) = 1 \\ x \leq 0 & \theta(x) = 0 \end{cases}$$

The free evolution of each unit is a slow increase during many time steps followed by a jump (Fig.12).

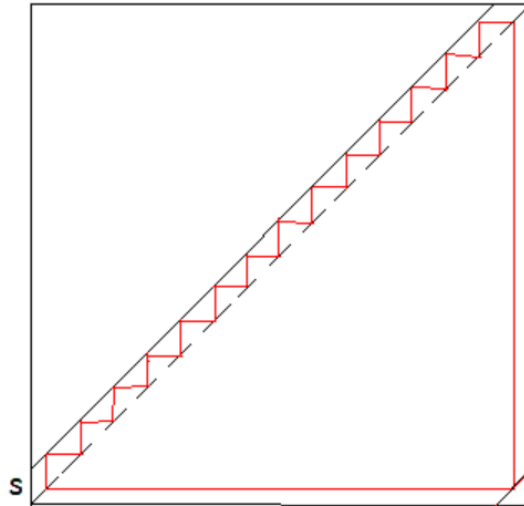


Figure 12: The "integrate and fire" free evolution

This jump is, by a neuron analogy [6], interpreted as a spike and the interaction with the other units occurs only when they spike. In the Fig.13 we display the time evolution of the spiking units obtained for $k = 0, 0.5, 1.2$ and 1.5 . The simulations are run from random initial conditions in the unit interval and the s_i 's are also chosen at random.

As the coupling increases one sees an increase in the spiking rate but not special coordination between the firing times. However, above around $k = 1$ a distinct clustering of the spiking patterns is clearly observed. How these correlations may be characterized will later be seen.

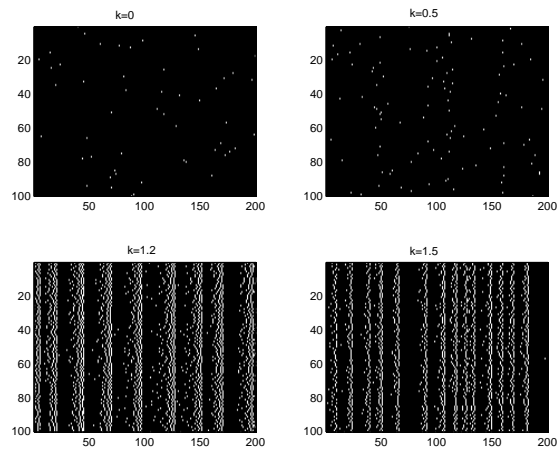


Figure 13: Spiking patterns for different coupling values. 200 time steps, 100 units.

3 Tools to characterize correlations in collective dynamics

In this section we describe some tools which may, qualitative and quantitatively characterize correlations in collective dynamics. The emphasis is, as stated before, on the characterization of the nature of the correlations that occur before synchronization sets in or even in systems that never synchronize.

3.1 The geometry of the dynamics

Given a set of N time series one defines a distance between each pair. One possibility is to consider the Euclidean distance

$$d_{ij} = \frac{1}{T - t_0} \sqrt{\sum_{t=t_0}^T (x_i(t) - x_j(t))^2} \quad (10)$$

Then, using the technique of multidimensional scaling (MDS), imbed the N time series as points in an Euclidean space. MDS begins with a $N \times N$ distance matrix $D = \{d_{ij}\}$ and the aim is to find a configuration of points in a p -dimensional space such that the coordinates of the points yield a Euclidean distance matrix with elements which are as close as possible to the distances in the original distance matrix (but not exactly the same if the original distances are not Euclidean).

We proceed as follows: denote by Y the matrix of coordinates in the embedding p -dimensional Euclidean space

$$Y = \begin{pmatrix} y_{11} & y_{12} & \cdots & \cdots & y_{1p} \\ y_{21} & y_{22} & \cdots & \cdots & y_{2p} \\ \vdots & \vdots & \vdots & \vdots & \vdots \\ y_{N1} & y_{N2} & \cdots & \cdots & y_{Np} \end{pmatrix} \quad (11)$$

and consider the following decomposition of the squared distance matrix

$$d_{ij}^2 = \left| \vec{y}_i - \vec{y}_j \right|^2 = b_{ii} + b_{jj} - 2b_{ij} \quad (12)$$

Then, the elements of the $N \times N$ matrix B

$$B = YY^T \quad (13)$$

are recovered from

$$b_{ij} = -\frac{1}{2} \left\{ d_{ij}^2 - \frac{1}{n} \left(\sum_{j=1}^n d_{ij}^2 + \sum_{i=1}^n d_{ij}^2 - \frac{1}{n} \sum_{i,j=1}^n d_{ij}^2 \right) \right\} \quad (14)$$

where by a translation of the origin in \mathbb{R}^p one makes $\sum_{i=1}^N y_{ik} = 0$ for all k .

One diagonalizes the matrix B reconstructed by (14)

$$B = V\Lambda V^T \quad (15)$$

with $\Lambda = (\lambda_1 \cdots \lambda_n)$ ($\lambda_1 \geq \lambda_2 \geq \cdots \geq \lambda_N$) being the diagonal matrix of eigenvalues and $V = [V_1, \cdots, V_N]$ the matrix of normalized eigenvectors. Whenever the dimension p of the imbedding space is smaller than N the rank of B is p (with the last $N - p$ eigenvalues being zero). One may write

$$B = V^* \Lambda^* V^{*T} \quad (16)$$

where V^* contains the first p eigenvectors and Λ^* the first p eigenvalues. Then a solution for Y is $Y = V^* \Lambda^{*1/2}$.

When the input distance matrix is not Euclidean, the matrix B is not positive-definite. In such case, some of the eigenvalues of B will be negative and correspondingly some coordinate values will be complex numbers. If B has only a small number of small negative eigenvalues, it is still possible to use the eigenvectors associated with the p largest positive eigenvalues.

For the time series case, after the Euclidean embedding of the orbits is done, one obtains a cloud of points (a point for each orbit). The shape and effective dimension of the cloud is obtained by reducing the coordinates to the center of mass and computing the inertial tensor

$$T_{ij} = \sum_{k=1}^N y_i(k) y_j(k) \quad (17)$$

Let $\lambda(T)$ be the eigenvalues of T . Once the eigenvalues $\{\lambda_k\}$ and eigenvectors $\{V_k\}$ of T are found, the relevant quantities, to characterize the correlations, are the projections (x_i, V_k) of the coordinate vectors on the eigenvectors, in particular on those associated to the largest eigenvalues.

3.2 Dynamical clustering

Here one wants to develop a tool to detect the dynamical communities that emerge from the interaction. For this purpose the relevant quantities characterizing the dynamics of each agent are the coordinate increments

$$\Delta_i(t) = x_i(t) - x_i(t-1) \quad (18)$$

which may be used to find a dynamical distance of the agents

$$d_{ij} = \sqrt{\sum_{t=1}^T |\Delta_i(t) - \Delta_j(t)|^2} \quad (19)$$

From the distances one defines an adjacency matrix

$$A_{ij} = \exp(-\beta(d_{ij} - d_{\min})) \quad (20)$$

a degree matrix

$$(G)_{ii} = \sum_{j \neq i} A_{ij} \quad (21)$$

and a Laplacian matrix

$$L = G - A \quad (22)$$

The lowest eigenvalues in the L -spectrum provide information on the dynamical communities insofar as they minimize the RatioCut of K communities [60]

$$\text{RatioCut}(C_1, \dots, C_K) = \frac{1}{2} \sum_{k=1}^K \frac{W(C_k, \overline{C_k})}{|C_k|} \quad (23)$$

with $W(C_k, \overline{C_k}) = \sum_{i \in C_k, j \in \overline{C_k}} A_{ij}$ being the sum of the external connections of the community C_k , and $|C_k|$ the number of elements in the C_k community.

3.3 The conditional Lyapunov spectrum

An issue of some relevance in multi-agent systems is to compare the view that each agent has of its dependence on the dynamics of the other agents with the actual dependence on the dynamics of the whole network. This is captured by the notion of *conditional exponents*. Conditional exponents, first introduced by Pecora and Carroll [34] in their study of synchronization of chaotic systems, have been shown to be good ergodic invariants [61], playing an important role as self-organization parameters [62]. The conditional exponents are computed in a way similar to the Lyapunov exponents but with each agent taking into account only its neighbors, not the whole system. However for the time average required for the calculation of the ergodic invariants, the actual global dynamics is used.

For a system with the neighborhood degree characterized by the adjacency matrix, the calculation of the conditional exponents spectrum is equivalent to the computation of the Jacobian of a modified dynamics where the interaction is weighed by the proximity of the agents (that is, by the adjacency matrix). Nevertheless the Jacobian is averaged over the orbits of the actual dynamics. For example, for the interacting oscillators of the deformed Kuramoto model, the Jacobian would be computed for a fictitious dynamics

$$x_i(t+1) = x_i(t) + \omega_i + \frac{K}{N-1} \sum_{j=1}^N A_{ij} \pi f^{(n)}(x_j - x_i) \quad (24)$$

The integrated difference of the the conditional and the Lyapunov spectrum is an important parameter to characterize the correlated dynamics.

Another promising technique to characterize the correlations occurring before synchronization has been developed by Lopez and Rodriguez [39] who, by considering the Hilbert transform of the coupled time series, obtain an evolving phase and then compute the entropy of the phase distribution. We will not deal here with this technique and refer to [39] for details.

How the above techniques do indeed provide information on the correlations of the collective dynamics will be clear by their application to the models described in Section 2.

4 Illustration of the tools on the model interactions

4.1 The deformed Kuramoto model

4.1.1 The geometry of the dynamics

We have applied the geometrical technique to the model (2), the distance of agent i to agent j being the sum of the distances on the circle on the last 100 time steps. Embedding each 100–times orbit as points in Euclidean space and using MDS, the eigenvalues $\lambda(B)$ of the B matrix were obtained.

The coordinates of the imbedded dynamics are then reduced to the center of mass and the inertial tensor is computed,

$$T_{ij} = \sum_{k=1}^N y_i(k)y_j(k) \quad (25)$$

the eigenvalues $\{\lambda_k(T)\}$ being the eigenvalues of T and $\{V_k\}$ its eigenvectors.

Figs. 14 and 19 show the results of the geometrical analysis for the dynamics of the model (2). Figs. 14, 16 and 18 show the eigenvalues of the B and T matrices and Figs. 15, 17 and 19 the projection of the dynamics on the first and second eigenvectors of T . Of particular interest is the fast reduction in the geometrical dimension of the dynamics, as measured by the fast convergence to zero of the $\lambda(T)$ eigenvalues, for $K \neq 0$. The whole dynamics seems to be approximately embedded in a two-dimensional subspace. Therefore, the projections on the first two (dominant) eigenvectors which display very distinct organized patterns, exhibit the strong correlations that already exist before synchronization sets in.

The projection of the embedded coordinates $\{x_i\}$ on the eigenvectors V_k associated to the largest eigenvalues of T may be considered as the new order parameters that characterize the correlations that occur before synchronization. Of interest are also the parameters $P_k = \sum_{i=1}^N |(x_i, V_k)|$.

4.1.2 Dynamical clustering

Distances and adjacency matrices were computed from the coordinate increments (Eqs.18 to 21). In Figs. 20, 21 and 22 we have plotted the spectrum of the Laplacian matrix L as well as the structure of the second and third eigenvectors to show the nature of the dominant communities.

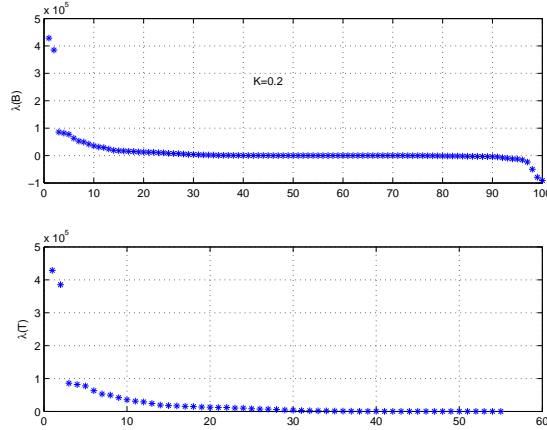


Figure 14: Eigenvalues of the B (Eq.13) and T (Eq.17) matrices for $K = 0.2$

4.1.3 The conditional exponents spectrum

As explained before, the conditional exponents are obtained from the Jacobian weighed by the agents proximity (that is, by the adjacency matrix) averaged over the orbits of the actual dynamics. For the deformed Kuramoto model, the Jacobian is computed for a fictitious dynamics

$$x_i(t+1) = x_i(t) + \omega_i + \frac{K}{N-1} \sum_{j=1}^N A_{ij} \pi f^{(n)}(x_j - x_i) \quad (26)$$

The adjacency matrix that is used is the same that was derived in the previous subsection (4.1.2).

In Figs. 23, 24 and 25 the the spectrum of the Lyapunov number ($\mu_i = e^{\lambda_i}$) of the system (2) is compared with the conditional number ($\mu_i^C = e^{\lambda_i^C}$) spectrum for $K = 0.2, 0.4$ and 0.8 .

One sees that for small coupling the conditional number spectrum is still close to the spectrum of the uncoupled system, meaning that the "perception" of the agents is very close to a situation where their dynamics looks as a free dynamics, although in fact it is already fully correlated, as evidenced by the Lyapunov spectrum. As the coupling increases the conditional number spectrum becomes closer and closer to the Lyapunov spectrum. The integrated difference of the two spectra is an important parameter to characterize the correlated dynamics.

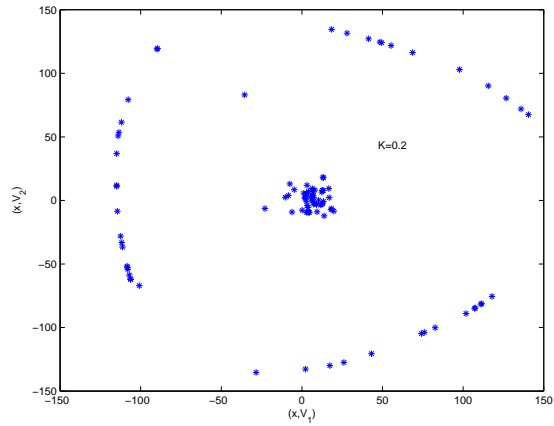


Figure 15: Projection of the dynamics on the first and second eigenvectors for $K = 0.2$

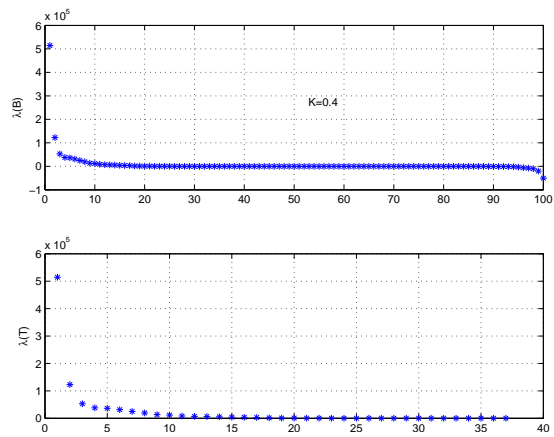


Figure 16: Eigenvalues of the B (Eq.13) and T (Eq.17) matrices for $K = 0.4$

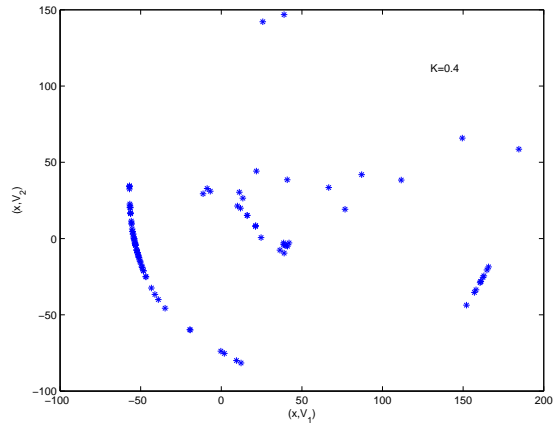


Figure 17: Projection of the dynamics on the first and second eigenvectors for $K = 0.4$

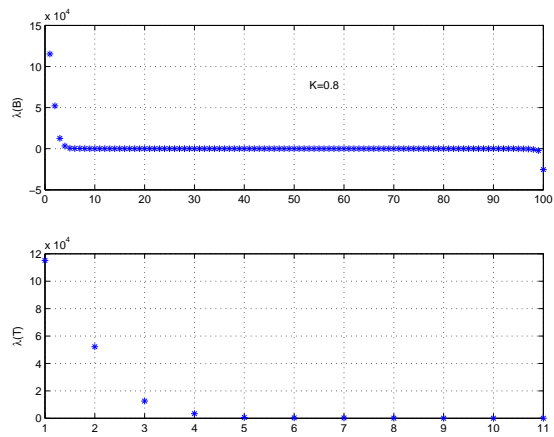


Figure 18: Eigenvalues of the B (Eq.13) and T (Eq.17) matrices for $K = 0.8$

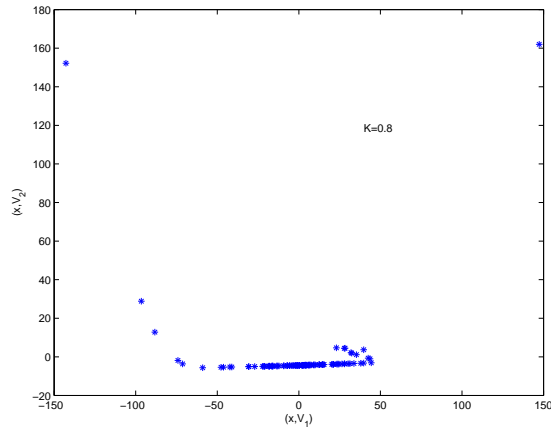


Figure 19: Projection of the dynamics on the first and second eigenvectors for $K = 0.8$

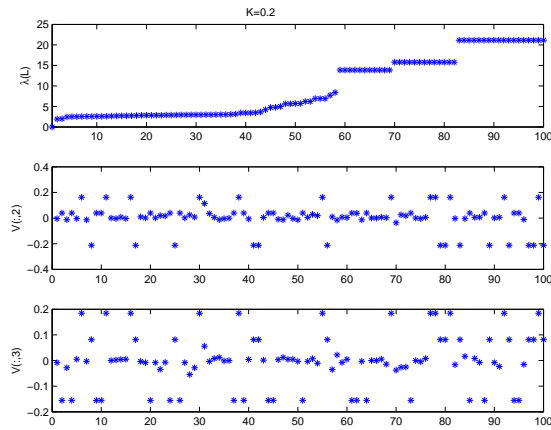


Figure 20: The spectrum of the Laplacian matrix L and the second and third eigenvectors ($K = 0.2$)

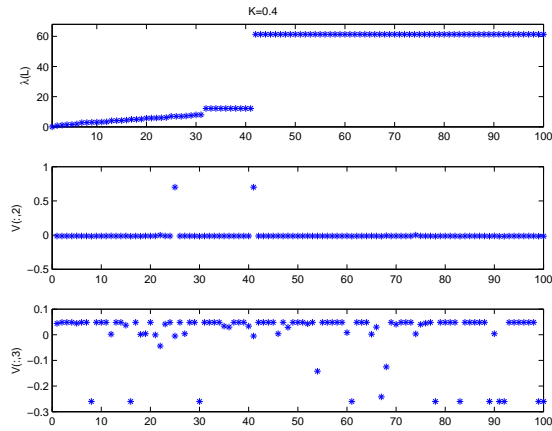


Figure 21: The spectrum of the Laplacian matrix L and the second and third eigenvectors ($K = 0.4$)

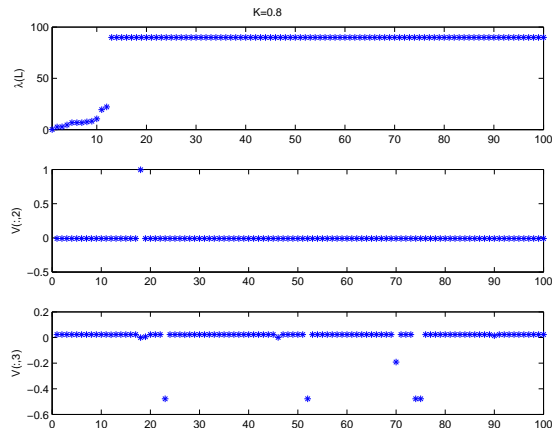


Figure 22: The spectrum of the Laplacian matrix L and the second and third eigenvectors ($K = 0.8$)

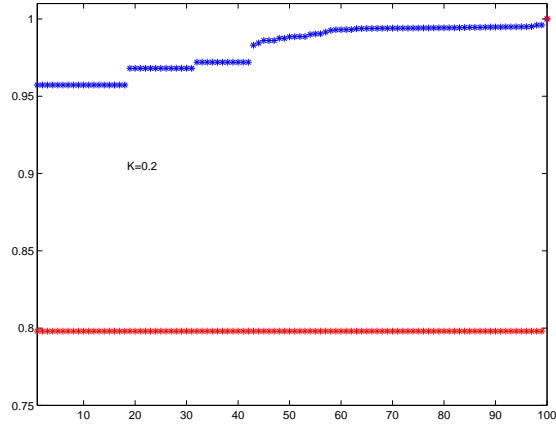


Figure 23: Conditional (blue) versus Lyapunov (red) numbers ($K = 0.2$)

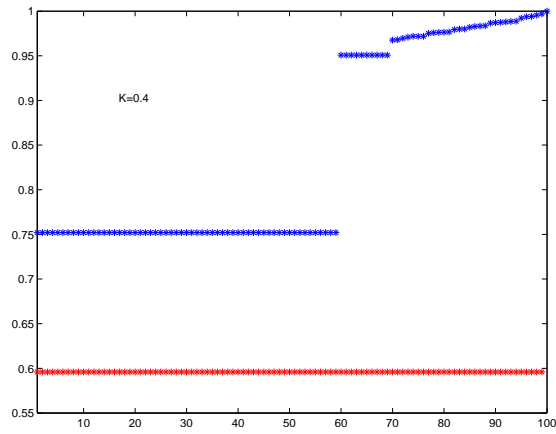


Figure 24: Conditional (blue) versus Lyapunov (red) numbers ($K = 0.4$)

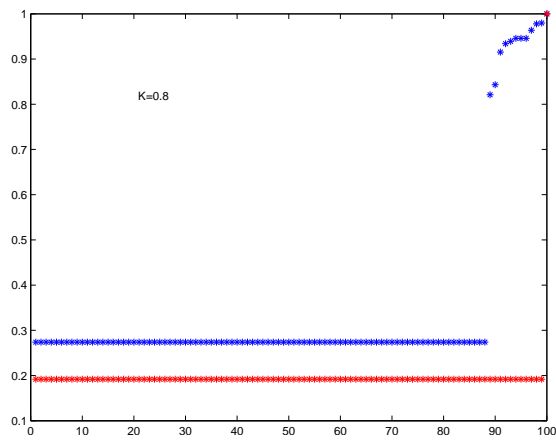


Figure 25: Conditional (blue) versus Lyapunov (red) numbers ($K = 0.8$)

4.2 The triangle interaction model

For the triangle interaction, the dynamical dimension reduction is not as dramatic as in the deformed Kuramoto model, as is evident from the behavior of its Lyapunov spectrum (Fig. 11). Therefore one expects the correlations to develop at a slower pace as the coupling (K) increases.

4.2.1 The geometry of the dynamics

In the absence of interaction ($K = 0$) the inertial tensor has many large eigenvalues and the projections of the orbits on the two largest eigenvectors show no distinctive pattern (Fig. 26).

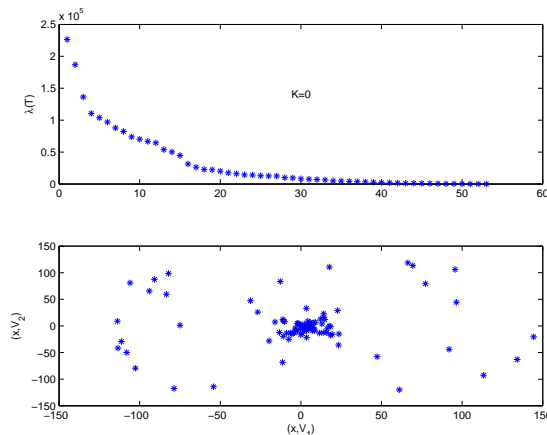


Figure 26: Eigenvalues of the matrix T and projection of the dynamics on the first and second eigenvectors for $K = 0$ (triangle interaction)

One sees that the case $K = 0.1$ (Figs. 27 and 28) is not very different from the $K = 0$ case, showing that strong correlations have not yet developed.

It is only for $K = 0.3$ and 0.7 that the dynamics is almost two dimensional and strongly correlated (Figs. 29, 30, 31 and 32).

4.2.2 Dynamical clustering

As before the dynamical distances and the adjacency matrix are obtained from the coordinate increments. The spectrum of the Laplacian matrix L and the second and third eigenvectors for $K = 0.1, 0.3$ and 0.7 are displayed in the Figs. 33, 33 and 33. Some information is obtained from these results, mostly for $K = 0.3$ and 0.7 , however the analysis of the geometry of the dynamics performed in the previous subsection seems to be, in this case, a better way to characterize the correlations.

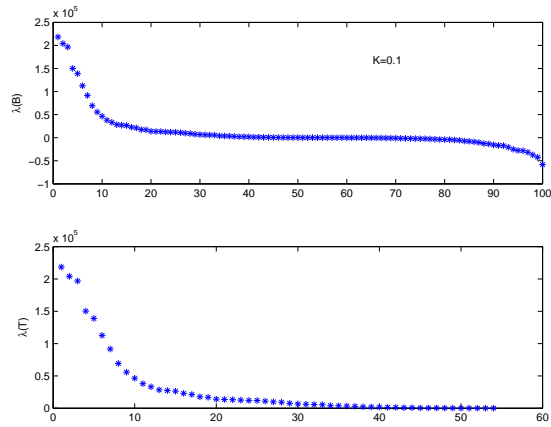


Figure 27: Eigenvalues of the B and T matrices for $K = 0.1$ (triangle interaction)

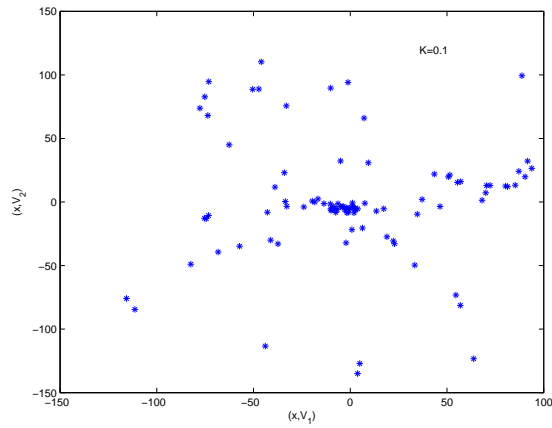


Figure 28: Projection of the dynamics on the first and second eigenvectors for $K = 0.1$ (triangle interaction)

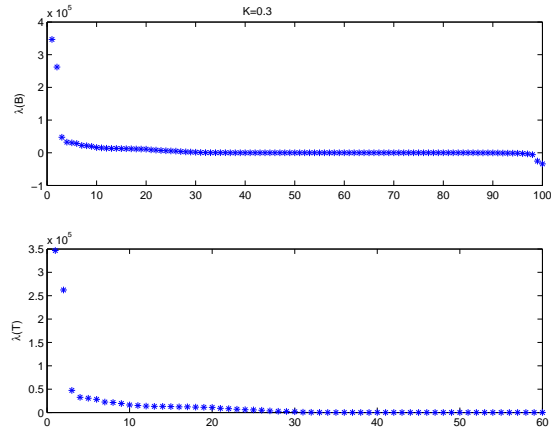


Figure 29: Eigenvalues of the B and T matrices for $K = 0.3$ (triangle interaction)

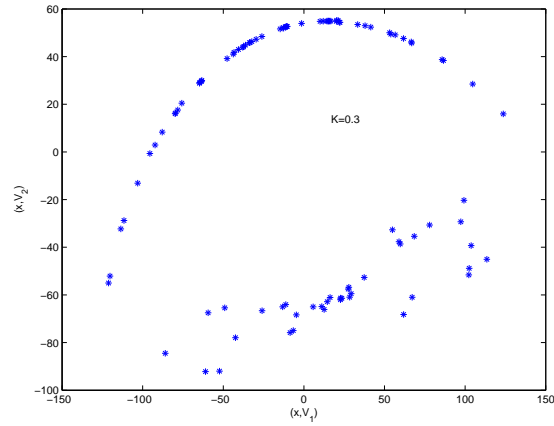


Figure 30: Projection of the dynamics on the first and second eigenvectors for $K = 0.3$ (triangle interaction)

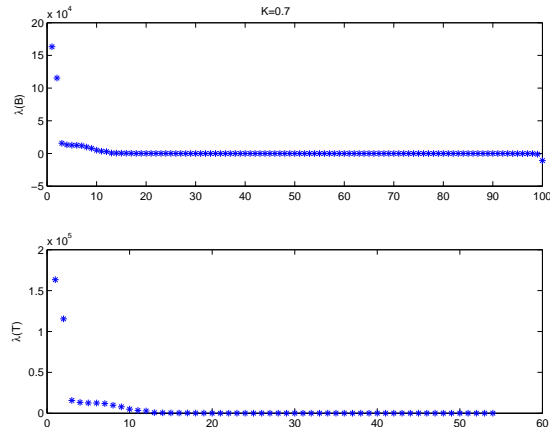


Figure 31: Eigenvalues of the B and T matrices for $K = 0.7$ (triangle interaction)

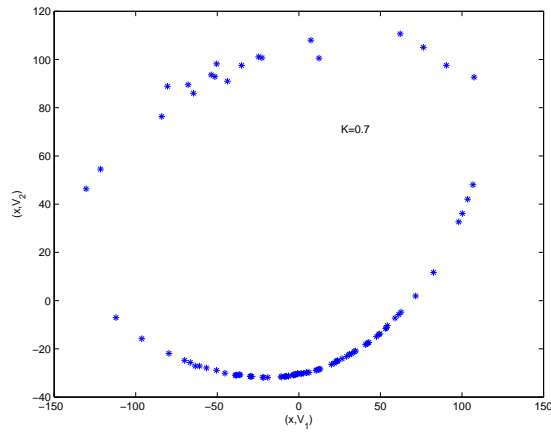


Figure 32: Projection of the dynamics on the first and second eigenvectors for $K = 0.7$ (triangle interaction)

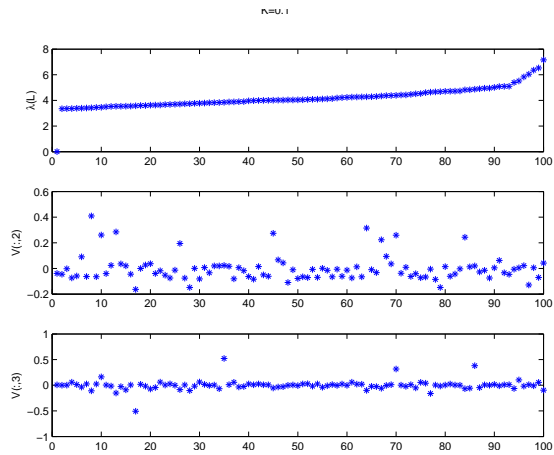


Figure 33: The spectrum of the Laplacian matrix L and the second and third eigenvectors for $K = 0.1$ (triangle interaction)

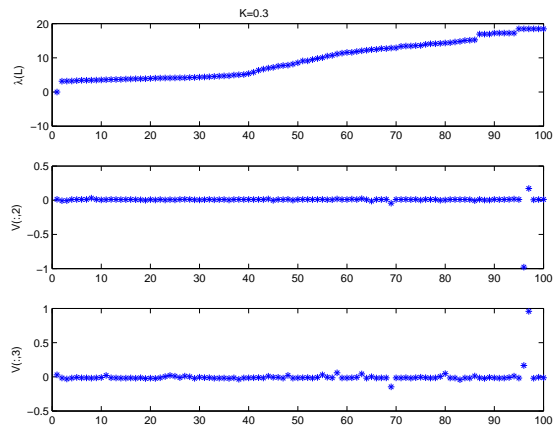


Figure 34: The spectrum of the Laplacian matrix L and the second and third eigenvectors for $K = 0.3$ (triangle interaction)

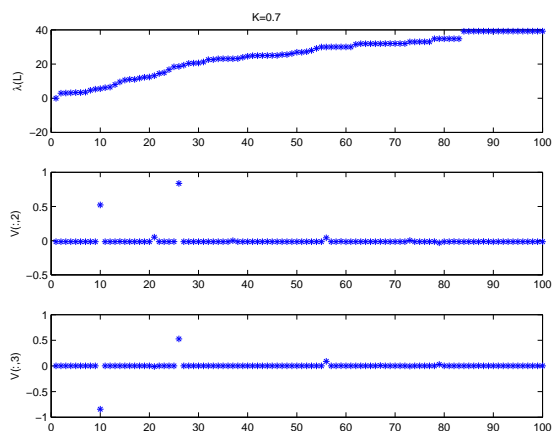


Figure 35: The spectrum of the Laplacian matrix L and the second and third eigenvectors for $K = 0.7$ (triangle interaction)

4.3 The deterministic integrate-and-fire model

The deterministic integrate-and-fire model is of a different nature as compared to the two previous models. It suggests that in addition to the geometric and clustering methods, that are fairly successful for continuous variable models, other tools should be developed to handle pulsing systems of this type.

To put into evidence the firing patterns we have displayed the histograms of the firing delays (Fig. 36). Here we define the firing delays as the separation in time of each firing with the closest firing in any one of the other units.

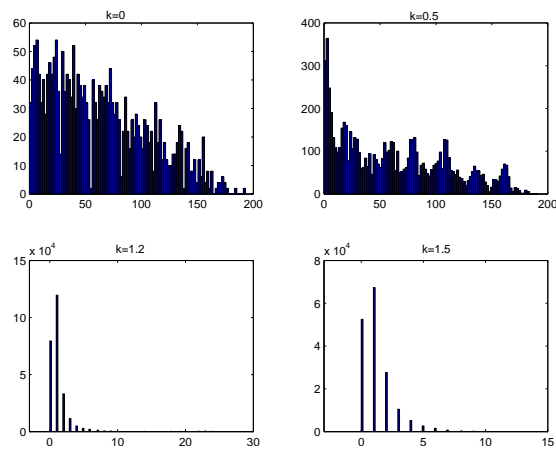


Figure 36: Histograms of the firing delays

One sees a tendency to organization of the system on the concentration of the distribution towards smaller delays on passing from $k = 0$ to $k = 0.5$, but it only only after $k \approx 1$ that the firings organize into a set of well defined patterns.

From the firing delays a distance between the units may be defined by the mean of the delays between each pair of units. From the distances an adjacency matrix was constructed and the spectrum of the Laplacian matrix computed (Fig. 37). Some information on the firing clusters is indeed obtained for $k = 1.2$ and 1.5 , however the information provided by the histograms of the firing delays is sharper.

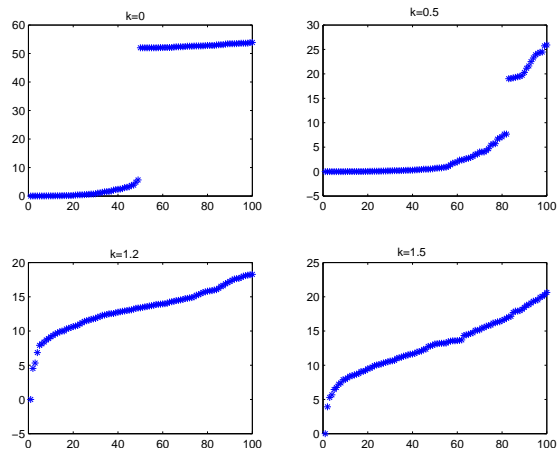


Figure 37: The Laplacian matrix spectrum

5 Conclusion

From the models analyzed in this paper it is clear that, in addition to synchronization, other types of strongly correlated behavior emerge in the collective dynamics of interacting systems. What at times has been dismissed as incoherent behavior contains important collective phenomena that enslave the dynamics. Hence, it seems important to develop tools which might be able to characterize qualitative and quantitatively the collective correlation effects that emerge before or instead of synchronization. A first step in this direction has been taken in this paper using geometrical and ergodic techniques.

References

- [1] A. Pikovsky, M. Rosenblum, J. Kurths; *Synchronization: a universal concept in nonlinear sciences*, Cambridge University Press 2001.
- [2] A. Pikovsky and M. Rosenblum; *Dynamics of globally coupled oscillators: Progress and perspectives*, Chaos 25 (2015) 097616.
- [3] C. W. Wu; *Synchronization in Complex Networks of Nonlinear Dynamical Systems*, World Scientific, Singapore 2007.
- [4] L. Kocarev (Ed.); *Consensus and Synchronization in Complex Networks*, Springer, Berlin 2013.
- [5] A. C. J. Luo; *Dynamical System Synchronization*, Springer 2013.
- [6] C. Aguirre, D. Campos, P. Pascual and E. Serrano; *Synchronization effects using a piecewise linear map-based spiking bursting neuron model*, Neurocomputing 69 (2006) 1116-1119.
- [7] A. A. Koronovskii, O. I. Moskalenko, V. I. Ponomarenko, M. D. Prokhorov, A. E. Hramov; *Binary generalized synchronization*, Chaos, Solitons and Fractals 83 (2016) 133-139.
- [8] L. Glass, *Synchronization and rhythmic processes in physiology*, Nature 410 (2001) 277-284.
- [9] D. L. Hayes, S. J. Asirvatham and P. A. Friedman; *Cardiac Pacing, Defibrillation and Resynchronization: A Clinical Approach*, Wiley-Blackwell, Chichester 2013.
- [10] Z. Lu, K. Klein-Cardena, S. Lee, T. M. Antonsen, M. Girvan and E. Ott; *Resynchronization of circadian oscillators and the east-west asymmetry of jet-lag*, Chaos 26 (2016) 094811.
- [11] A. Schnitzler and J. Gross; *Normal and pathological oscillatory communication in the brain*, Nature Reviews - Neuroscience 6 (2005) 285-295.

- [12] G. J. Ortega, L. M. de la Prida, R. G. Sola and J. Pastor; *Synchronization clusters of interictal activity in the lateral temporal cortex of epileptic patients: Intraoperative electrocorticographic analysis*, *Epilepsia* 49 (2008) 269-280.
- [13] A. A. Ioannides, V. Poghosyan, J. Dammers and M. Streit; *Real-time neural activity and connectivity in healthy individuals and schizophrenia patients*, *NeuroImage* 23 (2004) 473-482.
- [14] A. Sawa and S. H. Snyder; *Schizophrenia: Diverse approaches to a complex disease*, *Science* 296 (2002) 692-695.
- [15] P. R. Roelfsema, A. K. Engel, P. König and W. Singer; *Visuomotor integration is associated with zero time-lag synchronization among cortical areas*, *Nature* 385 (1997) 157-161.
- [16] J.-P. Lachaux, E. Rodriguez, J. Martinerie and F. J. Varela; *Measuring phase synchrony in brain signals*, *Human Brain Mapping* 8 (1999) 194-208.
- [17] M. A. Long, C. E. Landisman and B. W. Connors; *Small Clusters of Electrically Coupled Neurons Generate Synchronous Rhythms in the Thalamic Reticular Nucleus*, *The Journal of Neuroscience* 24 (2004) 341-349.
- [18] J. Buck; *Synchronous rhythmic flashing of fireflies*, *The Quarterly Review of Biology* 63 (1988) 265-289.
- [19] E. Rodriguez, N. George, J.-P. Lachaux, J. Martinerie, B. Renault and F. Varela; *Perception's shadow: long-distance synchronization of human brain activity*, *Nature* 397 (1999) 430-433.
- [20] F. Varela, J.-P. Lachaux, E. Rodriguez and J. Martinerie, *The brainweb: phase synchronization and large-scale integration*, *Nature Reviews Neuroscience* 2 (2001) 229-239.
- [21] A. K. Engel and W. Singer; *Temporal binding and the neural correlates of sensory awareness*, *Trends in Cognitive Sciences* 5 (2001) 16-25.
- [22] D. Malagarriga, M. A. García-Vellisca, A. E. P. Villa, J. M. Buldú, J. García-Ojalvo and A. J. Pons; *Synchronization-based computation through networks of coupled oscillators*, *Frontiers in Computational Neuroscience* 9:97, 2015.
- [23] G. Manzano, F. Galve, G. L. Giorgi, E. Hernández-García and R. Zambrini; *Synchronization, quantum correlations and entanglement in oscillator networks*, *Scientific Reports* 3 : 1439 DOI: 10.1038/srep01439 1.
- [24] R. Sevilla-Escoboza, J. M. Buldú, S. Boccaletti, D. Papo, D.-U. Hwang, G. Huerta-Cuellar and R. Gutiérrez; *Experimental implementation of maximally synchronizable networks*, arXiv:1507.02551.

- [25] A. Navas, J. A. Villacorta-Atienza, I. Leyva, J. A. Almendral, I. Sendiña-Nadal and S. Boccaletti; *Effective centrality and explosive synchronization in complex networks*, Phys. Rev. E 92 (2015) 062820.
- [26] M. Golubitsky and I. Stewart; *Rigid patterns of synchrony for equilibria and periodic cycles in network dynamics*, Chaos 26 (2016) 094803.
- [27] B. Ottino-Löffler and S. H. Strogatz; *Frequency spirals*, Chaos 26 (2016) 094804.
- [28] P. S. Skardal, D. Taylor and J. Sun; *Optimal synchronization of directed complex networks*, Chaos 26 (2016) 094807.
- [29] L. Wang and G. Chen; *Synchronization of multi-agent systems with metric-topological interactions*, Chaos 26 (2016) 094809.
- [30] J. Emenheiser, A. Chapman, M. Pósfai, J. P. Crutchfield, M. Mesbahi and R. M. D'Souza; *Patterns of patterns of synchronization: Noise induced attractor switching in rings of coupled nonlinear oscillators*, Chaos 26 (2016) 094816.
- [31] V. V. Makarova, A. A. Koronovskii, V. A. Maksimenko, A. E. Hramov, O. I. Moskalenko, J. M. Buldú and S. Boccaletti; *Emergence of a multilayer structure in adaptive networks of phase oscillators*, Chaos, Solitons and Fractals 84 (2016) 23-30.
- [32] R. Sevilla-Escoboza, I. Sendiña-Nadal, I. Leyva, R. Gutiérrez, J.M. Buldú and S. Boccaletti; *Inter-layer synchronization in multiplex networks*, arXiv: 1510.07498.
- [33] H. Fujisaka and T. Yamada; *Stability theory of synchronized motion in coupled-oscillator systems*, Prog. of Theor. Phys. 69 (1983) 32-47.
- [34] L. M. Pecora and T. L. Carroll; *Synchronization in chaotic systems*, Physical Review Letters 64 (1990) 821–824.
- [35] R. Vilela Mendes; *Clustering and synchronization with positive Lyapunov exponents*, Physics Letters A257 (1999) 132-138.
- [36] S. Boccaletti, J. Kurths, G. Osipov, D. L. Valladares and C. S. Zhou; *The synchronization of chaotic systems*, Physics Reports 366 (2002) 1–101.
- [37] L. M. Pecora and T. L. Carroll; *Synchronization of chaotic systems*, Chaos 25 (2015) 097611.
- [38] N. Fujiwara, J. Kurths and A. Díaz-Guilera; *Synchronization of mobile chaotic oscillator networks*, Chaos 26 (2016) 094824.
- [39] M. Lopez and F. Rodriguez; *Detection Method for Phase Synchronization in a Population of Spiking Neurons*, IWINAC 2013, Part I, LNCS 7930, J.M. Ferrández et al. (Eds.), pp. 421–431, Springer-Verlag Berlin Heidelberg 2013..

- [40] Y. Kuramoto and D. Battogtokh; *Coexistence of Coherence and Incoherence in Nonlocally Coupled Phase Oscillators*, Nonlinear Phenom. Complex Syst. 5 (2002) 380-385.
- [41] F. P. Kemeth, S. W. Haugland, L. Schmidt, I. G. Kevrekidis and K. Krischer; *A classification scheme for chimera states*, Chaos 26 (2016) 094815.
- [42] J. D. Hart, K. Bansal, T. E. Murphy and R. Roy; *Experimental observation of chimera and cluster states in a minimal globally coupled network*, Chaos 26 (2016) 094801.
- [43] D. M. Abrams and S. H. Strogatz; *Chimera States for Coupled Oscillators*, Phys. Rev. Lett. 93 (2004) 174102.
- [44] E. A. Martens, C. Bick and M. J. Panaggio; *Chimera states in two populations with heterogeneous phase-lag*, Chaos 26 (2016) 094819.
- [45] S. Nkomo, M. R. Tinsley and K. Showalter; *Chimera and chimera-like states in populations of nonlocally coupled homogeneous and heterogeneous chemical oscillators*, Chaos 26 (2016) 094826.
- [46] I. Franovic, K. Todorovic, N. Vasovic and N. Buric; *Cluster synchronization of spiking induced by noise and interaction delays in homogenous neuronal ensembles*, Chaos 22 (2012) 033147.
- [47] S. Jalan, A. Kumar, A. Zaikin and J. Kurths; *Interplay of degree correlations and cluster synchronization*, Phys. Rev. E 94 (2016) 062202.
- [48] M. T. Schaub, N. O'Clery, Y. N. Billeh, J.-C. Delvenne, R. Lambiotte and M. Barahona; *Graph partitions and cluster synchronization in networks of oscillators*, Chaos 26 (2016) 094821.
- [49] F. Sorrentino and L. Pecora; *Approximate cluster synchronization in networks with symmetries and parameter mismatches*, Chaos 26 (2016) 094823.
- [50] T. Nishikawa and A. E. Motter; *Network-complement transitions, symmetries, and cluster synchronization*, Chaos 26 (2016) 094818.
- [51] P. Ji, T. K. DM. Peron, F. A. Rodrigues and J. Kurths; *Analysis of cluster explosive synchronization in complex networks*, arXiv:1402.5587.
- [52] S. Watanabe and S. H. Strogatz, *Integrability of a Globally Coupled Oscillator Array*, Phys. Rev. Lett. 70 (1993) 2391-2394.
- [53] E. Ott and T. M. Antonsen; *Low dimensional behavior of large systems of globally coupled oscillators*, Chaos 18 (2008) 037113.
- [54] Y. Kuramoto; *Chemical Oscillations, Waves, and Turbulence*, Springer (1984)

- [55] S. H. Strogatz; *From Kuramoto to Crawford: exploring the onset of synchronization in populations of coupled oscillators*, Physica D 143 (2000) 1–20.
- [56] J. Acebrón, L. L. Bonilla, C. J. Pérez Vicente, F. Ritort and R. Spigler; *The Kuramoto model: A simple paradigm for synchronization phenomena*, Review of Modern Physics 77 (2005) 137–185
- [57] R. Vilela Mendes; *Tools for network dynamics* International Journal of Bifurcation and Chaos 15 (2005) 1185-1213.
- [58] J. G. Restrepo, E. Ott and B. R. Hunt; *Onset of synchronization in large networks of coupled oscillators*, Physical Review E 71 (2005) 036151.
- [59] R. Vilela Mendes; *Ergodic parameters and dynamical complexity*, Chaos 21 (2011) 037115.
- [60] U. Von Luxburg; *A tutorial on spectral clustering*, Stat. Comput. 17 (2007) 395-416.
- [61] R. Vilela Mendes; *Conditional exponents, entropies and a measure of dynamical self-organization*, Physics Letters A 248 (1998) 167.
- [62] R. Vilela Mendes; *Characterizing self-organization and coevolution by ergodic invariants*, Physica A 276 (2000) 550.